

# 1 A growing threat to the ozone layer from short-lived anthropogenic 2 chlorocarbons

3 David E. Oram (1,2), Matthew J. Ashfold (3), Johannes C. Laube (2), Lauren J. Gooch (2),  
4 Stephen Humphrey (2), William T. Sturges (2), Emma Leedham-Elvidge (2,8), Grant L. Forster  
5 (1,2), Neil R.P. Harris (4), Mohammed Iqbal Mead (4,5), Azizan Abu Samah (5), Siew Moi  
6 Phang (5), Chang-Feng Ou-Yang (6), Neng-Huei Lin (6), Jia-Lin Wang (7), Angela K. Baker  
7 (8), Carl A. M. Brenninkmeijer (8) and David Sherry (9)

8 (1) National Centre for Atmospheric Science, School of Environmental Sciences, University of  
9 East Anglia, Norwich, NR4 7TJ, UK (d.e.oram@uea.ac.uk); (2) Centre for Ocean and  
10 Atmospheric Sciences, School of Environmental Sciences, University of East Anglia, Norwich,  
11 UK; (3) School of Environmental and Geographical Sciences, University of Nottingham  
12 Malaysia Campus, 43500 Semenyih, Malaysia; (4) Centre for Atmospheric Informatics and  
13 Emissions Technology, School of Energy, Environment and Agrifood/Environmental  
14 Technology, Cranfield University, UK; (5) Institute of Ocean and Earth Sciences, University of  
15 Malaya, Kuala Lumpur, Malaysia; (6) Department of Atmospheric Sciences, National Central  
16 University, Taoyuan, Taiwan; (7) Department of Chemistry, National Central University,  
17 Taoyuan, Taiwan; (8) Max Planck Institute for Chemistry, Air Chemistry Division, Mainz,  
18 Germany; (9) Nolan Sherry & Associates, Kingston upon Thames, UK.

## 19 **Abstract**

20 Large and effective reductions in emissions of long-lived ozone-depleting substance (ODS)  
21 are being achieved through the Montreal Protocol, the effectiveness of which can be seen in  
22 the declining atmospheric abundances of many ODS. An important remaining uncertainty  
23 concerns the role of very short lived substances (VSLS) which, owing to their relatively short  
24 atmospheric lifetimes (less than 6 months), are not regulated under the Montreal Protocol.  
25 Recent studies have found an unexplained increase in the global tropospheric abundance of  
26 one VSLS, dichloromethane ( $\text{CH}_2\text{Cl}_2$ ), which has increased by around 60% over the past  
27 decade. Here we report dramatic enhancements of several chlorine-containing VSLS (Cl-  
28 VSLS), including  $\text{CH}_2\text{Cl}_2$  and  $\text{CH}_2\text{ClCH}_2\text{Cl}$  (1,2-dichloroethane), observed in surface and  
29 upper tropospheric air in East and South East Asia. Surface observations were, on occasion,  
30 an order of magnitude higher than previously reported in the marine boundary layer, whilst  
31 upper tropospheric data were up to 3 times higher than expected. In addition we provide  
32 further evidence of an atmospheric transport mechanism whereby substantial amounts of  
33 industrial pollution from East Asia, including these chlorinated VSLS, can rapidly, and  
34 regularly, be transported to tropical regions of the western Pacific and subsequently uplifted  
35 to the tropical upper troposphere. This latter region is a major provider for air entering the  
36 stratosphere and so this mechanism, in conjunction with increasing emissions of Cl-VSLS  
37 from East Asia, could potentially slow the expected recovery of stratospheric ozone.

## 38 **1. Introduction**

39 Large-scale ozone depletion in the stratosphere is a persisting global environmental problem.  
40 It is predominantly caused by the release of reactive chlorine and bromine species from  
41 halogenated organic compounds. Although the basic science is well established, there  
42 remains significant uncertainty surrounding the long-term recovery of the ozone layer (Hegglin  
43 et al., 2015). One important issue is the recent, unexplained increase in the global tropospheric  
44 abundance of dichloromethane ( $\text{CH}_2\text{Cl}_2$ ), which has increased by ~60% over the past decade  
45 (Leedham-Elvidge et al., 2015; Hossaini et al., 2015a; Carpenter and Reimann et al., 2015).

46 CH<sub>2</sub>Cl<sub>2</sub> is one of a large group of halogenated compounds known as VSLS (very short-lived  
47 substances). Owing to their relatively short atmospheric lifetimes (typically less than 6 months)  
48 and their correspondingly low Ozone Depletion Potentials (ODPs), VSLS are not currently  
49 regulated by the Montreal Protocol. It is however estimated that a significant fraction of VSLS  
50 and their atmospheric degradation products reach the stratosphere (>80% in the case of  
51 chlorinated VSLS; Carpenter and Reimann et al., 2015) and, furthermore, halogenated VSLS  
52 have been shown to have a disproportionately large impact on radiative forcing and climate  
53 due to their atmospheric breakdown, and the subsequent depletion of ozone, occurring at  
54 lower, climate sensitive altitudes (Hossaini et al., 2015b). According to the most recent  
55 Scientific Assessment of Stratospheric Ozone Depletion (Carpenter and Reimann et al., 2015)  
56 over the period 2008-2012 the total chlorine from VSLS increased at a rate of approximately  
57  $1.3 \pm 0.2$  ppt Cl yr<sup>-1</sup>, the majority of this increase being due to CH<sub>2</sub>Cl<sub>2</sub>, and this has already  
58 begun to offset the decline in total tropospheric chlorine loading over the same period ( $13.4 \pm$   
59  $0.9$  ppt Cl yr<sup>-1</sup>) caused by the reduced emissions of substances controlled by the Montreal  
60 Protocol.

61  
62 In recent years much attention has been focussed on the potential of bromine-containing  
63 VSLS to contribute to stratospheric ozone depletion (Law and Sturges, 2007; Montzka and  
64 Reimann, 2011). This is primarily due to the large observed discrepancy between the  
65 measured inorganic bromine in the stratosphere and the amount of bromine available from  
66 known, longer lived source gases, namely the halons and methyl bromide (Dorf et al., 2006).  
67 In contrast, the role of very short-lived chlorine compounds (Cl-VSLS) in ozone depletion has  
68 been considered relatively minor because they are believed to contribute only a few percent  
69 to the total chlorine input to the stratosphere, the majority of which is supplied by long-lived  
70 compounds such as the chlorofluorocarbons (CFCs), methyl chloroform (CH<sub>3</sub>CCl<sub>3</sub>) and carbon  
71 tetrachloride (CCl<sub>4</sub>). Since 1987 the consumption of these long-lived anthropogenic  
72 compounds has been controlled by the Montreal Protocol and the sum of total organic chlorine  
73 in the troposphere has been falling since its peak of around 3660 parts per trillion (ppt) in  
74 1993/94 to ~3300 ppt in 2012 (Carpenter and Reimann et al., 2015). Because of its relatively  
75 short atmospheric lifetime (~5 years) and its high chlorine content (3 chlorine atoms per  
76 molecule), the main contributor to this decline has been CH<sub>3</sub>CCl<sub>3</sub>. However, most CH<sub>3</sub>CCl<sub>3</sub>  
77 has now been removed from the atmosphere with a present day abundance of less than 5 ppt.  
78 Consequently the rate of decline in total organic chlorine has fallen to 13.4 ppt/year (2008-  
79 2012), which is around 50% smaller than the maximum seen in the late 1990s (Carpenter and  
80 Reimann et al., 2015).

81  
82 Owing to their short atmospheric lifetimes and their hitherto low background concentrations,  
83 chlorinated VSLS have not been considered of major importance for ozone depletion. Indeed  
84 the contribution of VSLS to the total chlorine entering the stratosphere is estimated to be only  
85 55 (38–95) ppt (Carpenter and Reimann et al., 2015), which is between 1% and 3% of the  
86 present day (2012) total (3300 ppt). However, because of their short lifetimes, the potential  
87 impact of VSLS on stratospheric ozone is highly dependent on the location of their sources,  
88 with emissions close to the major stratospheric input regions being of far greater significance  
89 for ozone depletion.

90  
91 The transport of trace gases and aerosols from the troposphere into the stratosphere occurs  
92 primarily in the tropics, where convective activity and vertical uplift are most intense. In order  
93 to get to the stratosphere an air parcel has to pass through the tropical tropopause layer (TTL),

94 the region of the atmosphere between the level of maximum convective outflow (~12 km  
95 altitude, 345K potential temperature) and the cold-point tropopause (~17 km, 380K) (see Box  
96 1-3, Figure 1 in Carpenter and Reimann et al., 2015). The vertical flux into the TTL is thought  
97 to be dominated by two main regional pathways, (1) ascent above the western Pacific during  
98 Northern Hemispheric (NH) winter and (2) the circulation of the Asian (Indian) Monsoon during  
99 NH summer (Fueglistaler et al., 2009). The latter has been suggested as the most important  
100 region for transport of anthropogenic pollution (Randel et al., 2010).

101  
102 Because of their short lifetimes, to be able to accurately determine the VSLS contribution to  
103 total organic halogen loading in the stratosphere it is highly desirable to collect data in the  
104 TTL. Surface measurements alone, particularly in regions outside the tropics where most long-  
105 term surface stations are sited, are not sufficient. Furthermore, because of the distribution and  
106 seasonality of stratospheric entry points it is also essential to measure in specific locations  
107 and at specific times of year, i.e. in the Indian summer monsoon and over the winter western  
108 Pacific. Unfortunately there are very few available measurements of VSLS in the TTL generally  
109 as it is above the maximum altitude of most research aircraft, and, furthermore, there is a  
110 paucity of both ground and aircraft data available in these two key regions of interest. Where  
111 recent TTL data is available it is primarily from different regions and focussed on brominated  
112 VSLS (e.g. Sala et al., 2014; Navarro et al., 2015).

113  
114 The focus of the present study is the western Pacific and, in particular, the region of the South  
115 China Sea. During NH winter the region is heavily influenced by the large anticyclone that  
116 forms over Siberia each year which gives rise to strong north-easterly winds that impact deep  
117 into the tropics as far south as Malaysia, Singapore and Indonesia. These north-easterly winds  
118 typically prevail for 4-5 months (November-March) and form part of the East Asian winter  
119 monsoon circulation. Superimposed on this seasonal synoptic flow are transient disturbances  
120 known as cold surges, which are triggered by a southward shift of the anticyclone and lead to  
121 sudden drops in surface air temperatures and increased wind speeds (Zhang et al., 1997;  
122 Garreaud, 2001). It has been proposed that during these events significant amounts of  
123 pollution from continental East Asia (>35°N) can be transported rapidly to the tropics (Ashfold  
124 et al., 2015). Furthermore, these events, which can last for many days, occur regularly each  
125 winter and are associated with some of the strongest convective activity in the western Pacific  
126 region. Indeed, trajectory calculations show that it can take less than 10 days for air masses  
127 to travel from the East Asian boundary layer (>35°N) to the upper tropical troposphere  
128 (altitudes > 200 hPa), thereby providing a fast route by which VSLS (and many other  
129 pollutants) may enter the lower stratosphere, despite their relatively short atmospheric  
130 lifetimes (Ashfold et al., 2015).

131  
132 Here we provide strong evidence to support this proposed transport mechanism based on new  
133 atmospheric observations in the East and SE Asia region. We will present new Cl-VSLS  
134 measurements from recent ground-based and aircraft campaigns in the region during which  
135 we have observed dramatic enhancements in a number of Cl-VSLS, including CH<sub>2</sub>Cl<sub>2</sub>, 1,2-  
136 dichloroethane (CH<sub>2</sub>ClCH<sub>2</sub>Cl), trichloromethane (CHCl<sub>3</sub>) and tetrachloroethene (C<sub>2</sub>Cl<sub>4</sub>).  
137 Furthermore we will demonstrate how pollution from China and the surrounding region can  
138 rapidly, and regularly, be transported across the South China Sea and subsequently uplifted  
139 to altitudes of 11-12 km, the region close to the lower TTL. Using the NAME particle dispersion  
140 model we will also investigate the origin of the observed Cl-VSLS and examine the frequency  
141 and duration of cold surge events. Finally we present some new estimates of CH<sub>2</sub>Cl<sub>2</sub>

142 emissions from East Asia and use these to estimate the likely emissions of  $\text{CH}_2\text{ClCH}_2\text{Cl}$ , for  
143 which there is little information in the recent literature.

144

## 145 **2. Methods**

146

147 Between 2012 and 2014, air samples were collected at various times at (1) two coastal sites  
148 in Taiwan, Hengchun (22.0547°N, 120.6995°E) and Fuguei Cape (25.297°N, 121.538°E); (2)  
149 the Bachok Marine Research Station on the Northeast coast of Peninsular Malaysia (6.009°N,  
150 102.425°E); and (3) during several flights of the IAGOS-CARIBIC aircraft between Germany  
151 and Thailand/Malaysia. IAGOS-CARIBIC is a European project making regular measurements  
152 from an in-service passenger aircraft operated by Lufthansa (Airbus A340-600;  
153 Brenninkmeijer et al., 2007; <http://www.caribic-atmospheric.com/>).

154

155 A total of 21 samples were collected at Hengchun between 7 March and 5 April 2013 with a  
156 further 22 samples taken at Cape Fuguei between 11 March and 4 April 2014. 28 samples  
157 were collected at Bachok between 20 January and 5 February 2014, during the period of the  
158 NE winter monsoon. The approximate location of each surface site is shown in Figure 1. The  
159 CARIBIC aircraft samples were collected during seven return flights between (i) Frankfurt  
160 (Germany) and Bangkok (Thailand), and (ii) Bangkok and Kuala Lumpur (Malaysia) during the  
161 periods December 2012 - March 2013 (4 flights) and November 2013 - January 2014 (3  
162 flights). All CARIBIC flights in this region between December 2012 and January 2014 have  
163 been included in this analysis. With the exception of 3 samples that were taken at altitudes  
164 between 8.5 and 9.8 km, the CARIBIC samples were all (n=179) collected at altitudes between  
165 10 and 12.3 km.

166

### 167 **2.1 Sample collection**

168 Air samples from Taiwan and Malaysia were collected in 3.2 litre silco-treated stainless steel  
169 canisters (Restek) at a pressure of approximately 2 bar using a battery-powered diaphragm  
170 pump (Air Dimensions, B series). In Taiwan the samples were collected from the surface via  
171 a 1 m x ¼" OD Dekabon sampling line, whilst in Bachok the samples were collected from the  
172 top of an 18 m tower via a 5 m x ¼" OD Dekabon sampling line. In both cases the tubing was  
173 flushed for at least 5 minutes prior to sampling. The sampling integrity was confirmed by  
174 sampling high purity air (BTCA-178, BOC) through the inlet tubing and pump. Samples were  
175 collected within 50 m of the sea and only when the prevailing winds were from the sea,  
176 minimising the impact of any local emissions. The CARIBIC aircraft samples were collected in  
177 2.7 litre glass flasks at a pressure of 4.5 bar using a two-stage metal bellows pumping system  
178 (Brenninkmeijer et al., 2007; Baker et al., 2010).

179

### 180 **2.2 Sample analysis**

181 The collected air samples were shipped to UEA and analysed for their halocarbon content by  
182 gas chromatography – mass spectrometry (GC-MS) following trace gas enrichment using  
183 previously published methods. All samples (i.e. Taiwan, Bachok and CARIBIC) were analysed  
184 for  $\text{CH}_2\text{Cl}_2$ ,  $\text{CHCl}_3$  and  $\text{C}_2\text{Cl}_4$  using an Entech-Agilent GC-MS system operating in electron  
185 ionisation (EI) mode, as described in Leedham-Elvidge et al., (2015). 1 litre samples were  
186 dried and pre-concentrated before injection onto a 30 m x 0.32 mm GS Gas Pro capillary  
187 column (Agilent), temperature ramped from -10°C to 200°C. Samples were interspersed with  
188 repeated analyses of a working standard (SX-706070), a high pressure air sample contained  
189 in a 34 litre electropolished stainless steel cylinder (Essex Industries) provided by the Earth

190 System Research Laboratory of the National Oceanic and Atmospheric Administration  
191 (NOAA-ESRL, Boulder, CO, USA).  $\text{CH}_2\text{Cl}_2$ ,  $\text{CHCl}_3$  and  $\text{C}_2\text{Cl}_4$  were quantified on ions with a  
192 mass-to-charge ratio of 84 ( $\text{CH}_2^{35}\text{Cl}_2^+$ ), 83 ( $\text{CH}^{35}\text{Cl}_2^+$  and  $\text{C}_2^{35}\text{Cl}_3^{37}\text{Cl}^+$ ) respectively. Mean  
193 analytical precisions were  $\pm 2\%$  for  $\text{CH}_2\text{Cl}_2$  and  $\text{C}_2\text{Cl}_4$ , and  $\pm 3\%$  for  $\text{CHCl}_3$ . Instrument blanks,  
194 determined by analysing 1 litre aliquots of high purity nitrogen (BOC, Research grade), were  
195 always below the detection limit of the instrument.

196  
197 Some of the ground-based samples and a subset of the CARIBIC samples were also analysed  
198 for a range of halocarbons, including the newly-identified  $\text{CH}_2\text{ClCH}_2\text{Cl}$ , using a pre-  
199 concentration/GC system coupled to a Waters AutoSpec magnetic sector MS instrument, also  
200 operating in EI mode, but run at a mass resolution of 1000 at 5 % peak height. Samples (using  
201 between 200 and 250 ml of air) were analysed on an identical GS GasPro column following a  
202 previously described method (Laube et al., 2010; Laube et al., 2012; Leedham-Elvidge et al.,  
203 2015).  $\text{CH}_2\text{ClCH}_2\text{Cl}$  was monitored on the ions with mass-to-charge ratios of 61.99 ( $\text{C}_2\text{H}_3^{35}\text{Cl}^+$ ,  
204 qualifier) and 63.99 ( $\text{C}_2\text{H}_3^{37}\text{Cl}^+$ , quantifier). Mean analytical precision was 1.4 % for  
205  $\text{CH}_2\text{ClCH}_2\text{Cl}$  and the average blank signal was 0.07 ppt (as quantified using regular  
206 measurements of research-grade helium) and was corrected for on a daily basis.

207  
208 **2.3 Calibration and quality assurance**  
209  $\text{CH}_2\text{Cl}_2$ ,  $\text{CHCl}_3$  and  $\text{C}_2\text{Cl}_4$  data are reported on the latest (2003) calibration scales provided by  
210 NOAA-ESRL. As was shown in Leedham-Elvidge et al., (2015) our  $\text{CH}_2\text{Cl}_2$  measurements  
211 compare very well with those of NOAA-ESRL at our mutual long-term sampling site at Cape  
212 Grim, Tasmania over more than 6 years. As a recognised international calibration scale for  
213  $\text{CH}_2\text{ClCH}_2\text{Cl}$  is not yet available this compound was calibrated at UEA using the established  
214 static dilution technique recently described (Laube et al., 2012).  $\text{CH}_2\text{ClCH}_2\text{Cl}$  was obtained  
215 from Sigma Aldrich with a stated purity of 99.8 %. Three dilutions were prepared at 7.1, 11.9  
216 and 15.8 ppt. The mixing ratio assigned to our working standard from these dilutions was 5.67  
217 ppt with a  $1 \sigma$  standard deviation of 1.8 %. CFC-11 was added to the dilutions as an internal  
218 reference compound and the CFC-11 mixing ratios assigned to the working standard through  
219 these dilutions agreed with the value assigned by NOAA-ESRL within 4.3 %. This is well within  
220 the estimated uncertainty of the calibration system of 7 % (Laube et al., 2012). In addition the  
221 mixing ratios of  $\text{CH}_2\text{ClCH}_2\text{Cl}$  in the working standard were compared with those in three other  
222 high-pressure canisters (internal surface was either electropolished stainless steel or  
223 passivated aluminium) over the whole measurement period. The ratios between standards did  
224 not change within the  $2 \sigma$  standard deviation of the measurements for any of the canisters  
225 analysed indicating very good long-term stability for  $\text{CH}_2\text{ClCH}_2\text{Cl}$ . This was also the case for  
226  $\text{CHCl}_3$  and  $\text{C}_2\text{Cl}_4$ . As noted in Leedham-Elvidge et al., (2015) mixing ratios of  $\text{CH}_2\text{Cl}_2$  were  
227 found to change over longer timescales in some of our standard canisters, but this drift has  
228 been successfully quantified and corrected for as indicated by the very good comparability  
229 with NOAA-ESRL measurements at the Cape Grim site noted above.

230  
231 **3. Results**  
232  
233 Figure 1 shows the location of the three surface observation stations as well as the location of  
234 the CARIBIC samples. The aircraft sampling points have been coloured by their  $\text{CH}_2\text{Cl}_2$   
235 concentration (see later discussion). Data from the surface stations and from the CARIBIC  
236 aircraft flights are summarised in Table 1, together with a summary of published observations  
237 as reported in the most recent Scientific Assessment of Stratospheric Ozone Depletion

238 (Carpenter and Reimann et al., 2015). It should be noted that  $\text{CH}_2\text{ClCH}_2\text{Cl}$  was only analysed  
239 for in selected samples and no data is available from Hengchun 2013 or from CARIBIC flights  
240 between Bangkok and Kuala Lumpur. In addition, only 16 Bachok samples were analysed for  
241  $\text{CH}_2\text{ClCH}_2\text{Cl}$ .

242  
243 The highest concentrations of chlorinated VSLs were measured in samples collected in  
244 Taiwan, suggesting that Taiwan is located relatively close to major emission regions. Figure 2  
245 shows the March/April 2014 data from Cape Fuguei. The Numerical Atmospheric-dispersion  
246 Modelling Environment model (NAME, see supplementary material) can be used to infer the  
247 recent transport history of this pollution. Our NAME analysis (Fig. 2 b-d) indicates that most of  
248 the samples that contained high concentrations of Cl-VSLs had originated from regions to the  
249 north of Taiwan, primarily the East Asian mainland. The median sum of chlorine from the 4  
250 VSLs listed above ( $\Sigma\text{Cl}_{\text{VSLs}}$ ) in 22 samples collected at Cape Fuguei in March/April 2014 was  
251 756 ppt (range 232-2178 ppt). Similarly high concentrations and variation were seen in the 21  
252 samples collected at Hengchun in March/April 2013 (Fig. S1 in the supplementary material).  
253 To put these concentrations in a global context, the total organic chlorine derived from all  
254 known source gases in the background troposphere (including CFCs, HCFCs, and longer-  
255 lived chlorocarbons) is currently around 3300 ppt, with a typical Cl-VSLs contribution in the  
256 remote marine boundary layer of approximately 3 % (Carpenter and Reimann et al., 2015).  
257 Of the four VSLs measured, the two largest contributors to  $\Sigma\text{Cl}_{\text{VSLs}}$  in Taiwan were  $\text{CH}_2\text{Cl}_2$   
258 (55-76 %) and  $\text{CH}_2\text{ClCH}_2\text{Cl}$  (14-30 %).

259  
260 Figure 3 shows the Cl-VSLs data from 28 samples collected at Bachok, Malaysia during the  
261 winter monsoon season in late January/ early February 2014. During this phase of the East  
262 Asian monsoon the prevailing winds are from the northeast and, as described earlier, are often  
263 impacted by emissions further to the north, including from mainland China. As can be seen in  
264 Figure 3, there was a 7 day period between 19 and 26 January when significantly enhanced  
265 concentrations of Cl-VSLs were observed. During this period NAME back trajectories show  
266 air travelling from continental East Asia and across the South China Sea before arriving at  
267 Bachok. Three examples during this cold surge event are shown in Fig. 3 (b-d). These  
268 trajectories often pass over Taiwan and, in some instances, also over parts of Indochina where  
269 additional emissions could have been picked up. As in the Taiwan samples,  $\text{CH}_2\text{Cl}_2$  is the  
270 largest contributor to  $\Sigma\text{Cl}_{\text{VSLs}}$  (59-66 %), having a mean concentration of  $179.9 \pm 71.9$  ppt  
271 (range 94.0 – 354.9 ppt, 9 samples) during the 7-day period of the pollution event. The mean  
272 concentration of  $\text{CH}_2\text{ClCH}_2\text{Cl}$  was  $64.4 \pm 23.9$  ppt (range 30.2 – 119.5 ppt), accounting for 19-  
273 23 % of  $\Sigma\text{Cl}_{\text{VSLs}}$ . These abundances are substantially higher than those typically found in the  
274 marine boundary layer. For example, the range of  $\Sigma\text{Cl}_{\text{VSLs}}$  from the 4 compounds listed above  
275 in the tropical marine boundary layer reported in WMO (2014) is 70-134 ppt. The range  
276 observed at Bachok over the entire sampling period was 207-1078 ppt, with medians of 546  
277 ppt and 243 ppt during the polluted (20-26 Jan) and less-polluted (27 Jan – 5 Feb) periods  
278 respectively (see Table 1). It is interesting to note that even in the period after the cold surge  
279 event (Fig.3 e,f), the levels of Cl-VSLs are still significantly higher than would be expected,  
280 suggesting that this region of the South China Sea is widely impacted by emissions from E  
281 Asia.

282  
283 The pollution or “cold surge” event observed at Bachok lasted for 6-7 days and the back  
284 trajectories shown in Figure 3 are typical of those arriving at Bachok during the winter  
285 monsoon period (see NAME animations in supplement). To further investigate the frequency

286 and typical duration of these events a NAME trajectory analysis using carbon monoxide (CO)  
287 as a tracer of industrial emissions from regions north of 20°N was conducted for the entire  
288 winter season (see supplementary information for details). Figure 4(a) shows a time series of  
289 this industrial CO tracer for winter 2013/2014 and suggests that the observed event in January,  
290 during which there was a strong correlation between the industrial CO tracer and CH<sub>2</sub>Cl<sub>2</sub> (Fig.  
291 4b), is likely to be repeated regularly throughout the winter. An analysis of a further 5 winters  
292 (Fig. 4c) demonstrates that 2013/14 was not unusual and that the events depicted in Figure  
293 3a occur repeatedly every year (Fig. S2 in the supplementary material).

294  
295 The Bachok measurements clearly demonstrate the rapid long-range transport of highly  
296 elevated concentrations of Cl-VSLS for several thousand kilometres across the South China  
297 Sea, as predicted by Ashfold et al., (2015). However, to have an impact on stratospheric ozone  
298 it is necessary to demonstrate that these high concentrations of Cl-VSLS can be rapidly lifted  
299 to the upper tropical troposphere (lower TTL) or above. Such evidence can be found in  
300 samples from several recent CARIBIC aircraft flights in the Southeast Asia region. Figure 1  
301 shows significant enhancements of CH<sub>2</sub>Cl<sub>2</sub> during flights over northern India and the Bay of  
302 Bengal, and also between Bangkok and Kuala Lumpur. The same data is plotted against  
303 longitude in Figure 5(a) which shows that elevated concentrations were observed in the seven  
304 CARIBIC flights in the region during the periods Dec 2012 - Mar 2013 and Nov 2013 - Jan  
305 2014. The samples were collected in the altitude range 10-12.3 km, showing that recent  
306 industrial emissions can regularly reach the lower boundary of the TTL. Although CH<sub>2</sub>CICH<sub>2</sub>Cl  
307 was only analysed for in a selection of samples during the flights from Germany to Bangkok,  
308 elevated mixing ratios coinciding with the high levels of CH<sub>2</sub>Cl<sub>2</sub> were clearly observed (Fig.  
309 5b). CHCl<sub>3</sub> and C<sub>2</sub>Cl<sub>4</sub> were also enhanced during these flights (Table 1), with ΣCl<sub>VSLs</sub> being in  
310 the range 48-330 ppt (Fig. 5c). This is up to 3.2 times higher than that previously found in the  
311 lower TTL (36-103 ppt; Carpenter and Reimann et al., 2015). The highest abundances of Cl-  
312 VSLS were seen in samples collected over the Bay of Bengal, and on flights between Bangkok  
313 and Kuala Lumpur (Fig. 5a). NAME back trajectories (Fig. 5d) indicate that in these cases the  
314 sampled air had almost always been transported from the east, and had often been impacted  
315 by emissions from East Asia, with possible contributions from other countries including the  
316 Philippines, Malaysia and Indochina.

317

#### 318 **4. Discussion**

319

320 The high mixing ratios of CH<sub>2</sub>Cl<sub>2</sub> observed in the Taiwan samples are not entirely unexpected.  
321 Previous studies have found very high levels (> 1 ppb) of CH<sub>2</sub>Cl<sub>2</sub> in various Chinese cities  
322 (Barletta et al., 2006) and in the Pearl River Delta region (Shao et al., 2011). Elevated levels  
323 (several hundred ppt) were also observed in aircraft measurements in polluted air emanating  
324 from China during the TRACE-P campaign in 2001 (Barletta et al., 2006). These studies took  
325 place in the early 2000s and emissions may be expected to have grown significantly since.  
326 CH<sub>2</sub>Cl<sub>2</sub> is predominantly (~90%) anthropogenic in origin, and is widely used as a chemical  
327 solvent, a paint stripper and as a degreasing agent (McCulloch and Midgeley, 1996; Montzka  
328 et al., 2011). Other uses include foam blowing and agricultural fumigation. A growing use of  
329 CH<sub>2</sub>Cl<sub>2</sub> is in the production of HFC-32 (CH<sub>2</sub>F<sub>2</sub>), an ozone friendly replacement for HCFC-22  
330 (CHF<sub>2</sub>Cl) in refrigeration applications. Around 10% of global CH<sub>2</sub>Cl<sub>2</sub> emissions come from  
331 natural marine and biomass burning sources (Simmonds et al., 2006; Montzka and Reimann  
332 et al., 2011).

333

334 Whilst the strong enhancements of  $\text{CH}_2\text{Cl}_2$  are not entirely unexpected, the presence of high  
335 concentrations of  $\text{CH}_2\text{ClCH}_2\text{Cl}$  most certainly are. There are very few previously reported  
336 measurements of  $\text{CH}_2\text{ClCH}_2\text{Cl}$ , particularly in recent years. Elevated levels have been  
337 observed in urban environments close to known emission sources (Singh et al., 1981) and,  
338 more recently, Xue et al., (2011) reported elevated levels ( $91 \pm 79$  ppt) in air samples collected  
339 in the boundary layer over north-eastern China in 2007. The few reported measurements of  
340  $\text{CH}_2\text{ClCH}_2\text{Cl}$  in the remote marine boundary layer are typically in the low ppt range (see Table  
341 1) but these were mostly made well over a decade ago. No long-term atmospheric  
342 measurements of  $\text{CH}_2\text{ClCH}_2\text{Cl}$  have been reported, and  $\text{CH}_2\text{ClCH}_2\text{Cl}$  is not reported by the  
343 main surface monitoring networks (AGAGE and NOAA), so current background  
344 concentrations and longer term trends are unknown.  $\text{CH}_2\text{ClCH}_2\text{Cl}$  is predominantly  
345 anthropogenic in origin, its primary use being in the manufacture of vinyl chloride, the  
346 precursor to polyvinyl chloride (PVC), and a number of chlorinated solvents.  $\text{CH}_2\text{ClCH}_2\text{Cl}$  also  
347 finds use as a solvent, dispersant and has historically been added to leaded petrol as a lead  
348 scavenger (EPA, 1984). In common with  $\text{CH}_2\text{Cl}_2$  it has also used as a cleaning/degreasing  
349 agent and as a fumigant. China is the world's largest producer of PVC accounting for 27% of  
350 global production in 2009 (DCE, 2017). Production has increased rapidly in recent years (14%  
351 per year over the period 2000-2009; DCE, 2017), which could potentially have led to increased  
352 atmospheric emissions of  $\text{CH}_2\text{ClCH}_2\text{Cl}$ . Simpson et al. (2011) observed a small enhancement  
353 in  $\text{CH}_2\text{ClCH}_2\text{Cl}$  in Canadian boreal forest fire plumes (background average, June-July 2008,  
354  $9.9 \pm 0.3$  ppt, plume average  $10.6 \pm 0.3$  ppt) and estimated a global boreal fire source of  $0.23$   
355  $\pm 0.19$  kilotonnes ( $\text{kt}$ )  $\text{yr}^{-1}$ .

356  
357 The other CI-VSLS presented here are  $\text{C}_2\text{Cl}_4$  and  $\text{CHCl}_3$ . In contrast to  $\text{CH}_2\text{ClCH}_2\text{Cl}$ , long-term  
358 atmospheric data records are available for these compounds, although there are few data  
359 from the SE Asia region. Current trends show that  $\text{C}_2\text{Cl}_4$  is declining in the background  
360 troposphere ( $\sim 6\%$   $\text{yr}^{-1}$ ), whilst  $\text{CHCl}_3$  is approximately constant (Carpenter and Reimann et  
361 al., 2015). However, both compounds were elevated in the samples containing high  
362 concentrations of  $\text{CH}_2\text{Cl}_2$  and  $\text{CH}_2\text{ClCH}_2\text{Cl}$ , suggesting that significant, co-located sources  
363 remain. Like  $\text{CH}_2\text{ClCH}_2\text{Cl}$ ,  $\text{C}_2\text{Cl}_4$  is almost exclusively anthropogenic in origin, used primarily  
364 as a solvent in the dry cleaning industry, as a metal degreasing agent and as a chemical  
365 intermediate, for example in the manufacture of the hydrofluorocarbons HFC-134a and HFC-  
366 125.  $\text{CHCl}_3$  is believed to be largely natural in origin (seawater, soils, macroalgae), but  
367 potential anthropogenic sources include the pulp and paper industry, water treatment facilities  
368 and HFC production (McCulloch, 2003; Worton et al., 2006; Montzka et al., 2011).

#### 369 370 *4.1 Regional emissions of $\text{CH}_2\text{Cl}_2$ and $\text{CH}_2\text{ClCH}_2\text{Cl}$*

371  
372 China does not report production or emission figures for  $\text{CH}_2\text{Cl}_2$ . However emissions of  $\text{CH}_2\text{Cl}_2$   
373 can be estimated from known Chinese production of HCFC-22 ( $\text{CHClF}_2$ ). This is possible  
374 because the production of HCFC-22 requires  $\text{CHCl}_3$  as feedstock (1 kg HCFC-22 requires 1.5  
375 kg  $\text{CHCl}_3$ ) and because  $\text{CHCl}_3$  is produced almost entirely (>99%) for HCFC-22 production.  
376 Production of chloromethanes by any manufacturing process leads to the inevitable co-  
377 production of  $\text{CH}_2\text{Cl}_2$  and  $\text{CHCl}_3$ , with smaller (3-5%) co-production of carbon tetrachloride  
378 ( $\text{CCl}_4$ ). The production ratios vary by individual plant but are within the range 30:70-70:30 (%  
379  $\text{CH}_2\text{Cl}_2$ : $\text{CHCl}_3$ ). Chinese chloromethanes plants, which together represent some 60% of global  
380 capacity and production, are generally built to a 40:60 - 60:40 flexibility ratio. With falling CFM  
381 demand due to diminished feedstock demand for HCFC-22 production, and based on regular



382 discussions with the individual large producers, ratios in China have been switching in recent  
383 years from the traditional 40:60 towards 50:50 ( $\text{CH}_2\text{Cl}_2$ : $\text{CHCl}_3$ ; Nolan Sherry 2016).

384

385 It can be calculated that in 2015 China produced approximately 600 kt of HCFC-22 for all uses  
386 (Nolan Sherry 2016), which would require 900 kt of  $\text{CHCl}_3$  as feedstock. By subtracting  
387 Chinese imports of  $\text{CHCl}_3$  (40 kt; Comtrade 2016) and allowing for some limited emissive  
388 solvent use (15 kt) suggests that China produced around 875 kt of  $\text{CHCl}_3$  in 2015. As noted  
389 above, in the chlorocarbon industry  $\text{CH}_2\text{Cl}_2$  and  $\text{CHCl}_3$  are produced in the same  
390 manufacturing process and in China this is currently moving from a historic production ratio of  
391 around 40:60 towards 50:50. Using a production ratio of 45:55 it can therefore be estimated  
392 that China produced around 715 kt of  $\text{CH}_2\text{Cl}_2$  in 2015. Approximately 90 kt of this was exported  
393 (Comtrade 2016) and another 170 kt was used for the production of HFC-32 ( $\text{CH}_2\text{F}_2$ ), which  
394 is a non-emissive application (Nolan Sherry 2016). This leaves an estimated 455 kt ( $\pm 10\%$ )  
395 of  $\text{CH}_2\text{Cl}_2$  which is used almost exclusively in emissive applications such as paint stripping,  
396 foam blowing, pharmaceuticals, solvent use, etc. Although there is no specific industry-based  
397 aggregation of these numbers, they have been verified in discussion with Chinese and other  
398 industry sources. A similar method has recently been used to assess emissions of  $\text{CCl}_4$   
399 (SPARC 2016).

400

401 There is a strong linear correlation between the observed  $\text{CH}_2\text{Cl}_2$  and  $\text{CH}_2\text{ClCH}_2\text{Cl}$  data at  
402 both Bachok ( $R^2 = 0.9799$ ) and Cape Fuguei ( $R^2 = 0.9189$ ). Combining the datasets yields a  
403 slope of  $0.4456 \pm 0.0194$  ( $R^2 = 0.9228$ ). Using the emissions for  $\text{CH}_2\text{Cl}_2$  derived above (455 kt)  
404 and making the assumptions that (1) all emissions originate in China and (2) there are no  
405 significant relative losses of the two compounds since emission (lifetimes are 144 days for  
406  $\text{CH}_2\text{Cl}_2$  and 65 days for  $\text{CH}_2\text{ClCH}_2\text{Cl}$ ) we can estimate Chinese emissions of  $\text{CH}_2\text{ClCH}_2\text{Cl}$  to  
407 be of the order of  $203 \pm 9 \text{ kt yr}^{-1}$ . If accurate, the scale of these emissions is a major surprise  
408 as  $\text{CH}_2\text{ClCH}_2\text{Cl}$  is highly toxic (suggesting that local emissions would be minimised) and  
409 believed to be used almost exclusively in non-emissive applications.

410

## 411 **5. Concluding remarks**

412

413 When calculating the VLSL contribution to stratospheric chlorine, it is usual to assume an  
414 average concentration in the region of the TTL known as the level of zero radiative heating  
415 (LZRH). The LZRH is located at the transition between clear-sky radiative cooling and clear-  
416 sky radiative heating. This occurs at an approximate altitude of 15 km and it is believed that  
417 air masses above this level will go on to enter the stratosphere (Carpenter and Reimann et  
418 al., 2015). As noted above there are very few measurements in this region and, furthermore,  
419 many of the available measurements were made over a decade ago and assumptions based  
420 on surface temporal trends have to be made in order to estimate present day values  
421 (Carpenter and Reimann et al., 2015; Hossaini et al., 2015). Another key deficiency in this  
422 estimation of VLSL concentrations entering the stratosphere is that most of the reported  
423 measurements have not been made in the two key regions where the strongest troposphere  
424 to stratosphere transport occurs. Although we have no data from the region of the LZRH, the  
425 CARIBIC data over northern India and SE Asia suggests that the contribution of VLSL to  
426 stratospheric chlorine loading may be significantly higher than is currently estimated (50-95  
427 ppt, Carpenter and Reimann et al., 2015). It is also interesting to note that the much-discussed  
428 contribution of VLSL-Br compounds to stratospheric bromine is approximately 5 ppt, which is  
429 equivalent to 300 ppt of chlorine (1 ppt of bromine is roughly equivalent to 60 ppt chlorine,

430 Sinnhuber et al., 2009). The CARIBIC measurements suggest that CI-VSLS could currently,  
431 on occasion, contribute a similar amount.

432

433 These new measurements of CI-VSLS in Taiwan, Malaysia and from an aircraft flying above  
434 South-East Asia show that there are substantial regional emissions of these compounds; that  
435 these emissions can be rapidly transported long distances into the deep tropics; and that an  
436 equally rapid vertical transport to the upper tropical troposphere is a regular occurrence.  
437 Although the focus of this paper is short-lived chlorinated gases, there are many other  
438 chemical pollutants contained in these air masses which will have a large impact on such  
439 things as regional air quality.

440

441 Unlike the bromine-containing VSLS which are largely natural in origin, the CI-VSLS reported  
442 here are mainly anthropogenic and consequently it would be possible to control their  
443 production and/or release to the atmosphere. Of particular concern are the rapidly growing  
444 emissions of  $\text{CH}_2\text{Cl}_2$ , and potentially  $\text{CH}_2\text{ClCH}_2\text{Cl}$ , especially when considering the  
445 geographical location of these emissions, close to the major uplift regions of the western  
446 Pacific (winter) and the Indian sub-continent (summer). Without a change in industrial  
447 practices the contribution of CI-VSLS to stratospheric chlorine loading is likely to increase  
448 substantially in the coming years, thereby endangering some of the hard-won gains achieved,  
449 and anticipated, under the Montreal Protocol.

450

#### 451 **References**

452 Ashfold, M.J., J.A. Pyle, A.D. Robinson, E. Meneguz, M.S.M. Nadzir, S.M. Phang, A.A.  
453 Samah, S. Ong, H.E. Ung, L.K. Peng, S.E. Young and N.R.P. Harris, Rapid transport of  
454 East Asian pollution to the deep tropics. *Atmos. Chem. Phys.*, **15**, 3565-  
455 3573, doi:10.5194/acp-15-3565-2015.

456 Baker, A.K., F. Slemr and C.A.M. Brenninkmeijer, Analysis of non-methane hydrocarbons in  
457 air samples collected aboard the CARIBIC passenger aircraft, *Atmos. Meas. Tech.*, **3**, 311-  
458 321, 2010.

459 Barletta, B., S. Meinardi, I.J. Simpson, F. S. Rowland, C-Y, Chan, X. Wang, S. Zou, L.Y. Chan  
460 and D.R. Blake, Ambient halocarbon mixing ratios in 45 Chinese cities, *Atmos. Environ.*,  
461 **40**, 7706-7719, doi:10.1016/j.atmosenv2006.08.039, 2006.

462 Bergman, J.W., E.J. Jensen, L. Pfister and Q. Yang, Seasonal differences of vertical-transport  
463 efficiency in the tropical tropopause layer: On the interplay between tropical deep  
464 convection, large-scale vertical ascent, and horizontal circulations, *J. Geophys. Res.*, **117**,  
465 D05302, doi:10.1029/2011JD016992, 2012.

466 Brenninkmeijer, C. A. M. *et al.*, Civil Aircraft for the regular investigation of the atmosphere  
467 based on an instrumented container: The new CARIBIC system. *Atmospheric Chemistry  
468 and Physics* **7**, 4953-4976 (2007).

469 Brioude, J., R.W. Portmann, J.S. Daniel, O.R. Cooper, G.J. Frost, K.H. Rosenlof, C. Granier,  
470 A.R. Ravishankara, S.A. Montzka and A. Stohl, Variations in ozone depletion potentials of  
471 very short-lived substances with season and emission region, *Geophys. Res. Lett.*, **37**,  
472 L19804, doi:10.1029/2010GL044856, 2010.

473 Carpenter L.J. and S. Reimann (Lead Authors), J.B. Burkholder, C. Clerbaux, B.D. Hall, R.  
474 Hossaini, J.C. Laube, and S.A. Yvon-Lewis, Ozone-depleting substances (ODSs) and other  
475 gases of interest to the Montreal Protocol, Chapter 1 in *Scientific Assessment of Ozone*

476 *Depletion: 2014*, Global Ozone Research and Monitoring Project – Report No. 55, World  
477 Meteorological Organization, Geneva, Switzerland, 2015.

478 Comtrade, <https://comtrade.un.org>, last accessed 25 May 2017.

479 DCE,  
480 [http://www.dce.com.cn/DCE/Education/Market%20Services/Resources/1514180/index.ht](http://www.dce.com.cn/DCE/Education/Market%20Services/Resources/1514180/index.html)  
481 [ml](http://www.dce.com.cn/DCE/Education/Market%20Services/Resources/1514180/index.html), Dalian Commodity Exchange website, PVC product guide, last accessed 24 May 2017.

482 Dorf, M., Butler, J. H., Butz, A., Camy-Peyret, C., Chipperfield, M. P., Kritten, L., Montzka, S.  
483 A., Simmes, B., Weidner, F., and Pfeilsticker, K.: Long-term observations of stratospheric  
484 bromine reveal slow down in growth, *Geophys. Res. Lett.*, **33**, L24803,  
485 doi:10.1029/2006GL027714, 2006.

486 EPA, Locating and estimating air emissions from sources of ethylene dichloride, Report of the  
487 United States Environmental Protection Agency, EPA-450/4-84-007d, March 1984.

488 Fueglistaler, S., M. Bonazzola, P.H. Haynes and T. Peter, Stratospheric water vapor predicted  
489 from the Lagrangian temperature history of air entering the stratosphere in the tropics, *J.*  
490 *Geophys. Res.*, **110**, D08107, doi:10.1029/2004JD005516, 2005.

491 Fueglistaler, S., A.E. Dessler, T.J. Dunkerton, I. Folkins, Q. Fu and P.W. Mote, Tropical  
492 tropopause layer, *Rev. Geophys.*, **47**, RG1004, doi:10.1029/2008RG000267, 2009.

493 Garreaud, R.D., Subtropical cold surges: regional aspects and global distribution, *Int. J.*  
494 *Climatol.*, **21**, 1181-1197, 2001.

495 Haines, P. E., and J. G. Esler, Determination of the source regions for surface to stratosphere  
496 transport: An Eulerian backtracking approach, *Geophys. Res. Lett.*, **41**, 1343–1349,  
497 doi:10.1002/2013GL058757, 2014.

498 Hegglin, M.I. (Lead Author), D.W. Fahey, M. McFarland, S.A. Montzka, and E.R. Nash, Twenty  
499 Questions and Answers About the Ozone Layer: 2014 Update, *Scientific Assessment of*  
500 *Ozone Depletion: 2014*, 84 pp., World Meteorological Organization, Geneva, Switzerland,  
501 2015.

502 Hossaini, R., M.P. Chipperfield, A. Saiz-Lopez, J.J. Harrison, R. von Glasow, R. Sommariva,  
503 E. Atlas, M. Navarro, S.A. Montzka, W. Feng, S. Dhomse, C. Harth, J. Mühle, C. Lunder,  
504 S. O'Doherty, D. Young, S. Reimann, M.K. Vollmer, P.B. Krummel and P.F. Bernarth,  
505 Growth in stratospheric chlorine from short-lived chemicals not controlled by the Montreal  
506 Protocol, *Geophys. Res. Lett.*, **42**, 4573-4580, doi:10.1002/2015GL063783, 2015(a).

507 Hossaini, R., M.P. Chipperfield, S.A. Montzka, A. Rap, S. Dhomse and W. Feng, Efficiency of  
508 short-lived halogens at influencing climate through depletion of stratospheric ozone. *Nature*  
509 *Geosci.*, **8**, 186-190, doi:10.1038/ngeo2363, 2015(b).

510 Law K.S. and W.T. Sturges (Lead authors), D.R. Blake, N.J. Blake, J.B. Burkholder, J.H.  
511 Butler, R.A. Cox, P.H. Haynes, M.K.W. Ko, K. Kreher, C. Mari, K. Pfeilsticker, J.M.C. Plane,  
512 R.J. Salawich, C. Schiller, B.-M. Sinnhuber, R. von Glasow, N.J. Warwick, D.J. Wuebbles  
513 and S.a. Yvon-Lewis, Halogenated very short lived substances, Chapter 2 in *Scientific*  
514 *Assessment of Ozone Depletion: 2006*, Global Ozone Research and Monitoring Project –  
515 Report No. 50, World Meteorological Organization, Geneva, Switzerland, 2007.

516 Laube, J.C., P. Martinerie, E. Witrant, T. Blunier, J. Schwander, C. A. M. Brenninkmeijer,  
517 T. J. Schuck, M. Bolder, T. Röckmann, C. van der Veen, H. Bönisch, A. Engel, G. P. Mills,  
518 M. J. Newland, D. E. Oram, C. E. Reeves and W. T. Sturges, Rapid growth of HFC-227ea  
519 (1,1,1,2,3,3,3-Heptafluoropropane) in the atmosphere, *Atmos. Chem. Phys.*, **10**, 5903-  
520 5910, 2010.

521 Laube, J.C., C. Hogan, M.J. Newland, F.S. Mani, P.J. Fraser, C.A.M. Brenninkmeijer, P.  
522 Martinerie, D.E. Oram, T. Röckmann, J. Schwander, E. Witrant, G.P. Mills, C.E. Reeves  
523 and W.T. Sturges, Distributions, long term trends and emissions of four perfluorocarbons

524 in remote parts of the atmosphere and firn air, *Atmos. Chem. Phys.*, **12**, 4081-4090, doi:10-  
525 5194/acp-12-4081-2012.

526 Leedham-Elvidge, E.C., D.E. Oram, J.C. Laube, A.K. Baker, S.A. Montzka, S. Humphrey, D.A.  
527 O'Sullivan, and C.A.M. Brenninkmeijer, Increasing concentrations of dichloromethane,  
528 CH<sub>2</sub>Cl<sub>2</sub>, inferred from CARIBIC air samples collected 1998–2012, *Atmos. Chem. Phys.* **15**,  
529 1939-1958, doi:10.5194/acp-15-1939-2015.

530 McCulloch, A. and P.M. Midgley, The production and global distribution of emissions of  
531 trichloroethene, tetrachloroethene and dichloromethane over the period 1988-1992, *Atmos.*  
532 *Environ.*, **30**, 601-608, 1996.

533 McCulloch, A., Chloroform in the environment: Occurrence, sources, sinks and effects,  
534 *Chemosphere*, **50** (10), 1291-1308, doi: 10.1016/S0045-6535(02)00697-5, 2003.

535 Montzka, S. A., S. Reimann (Lead Authors), A. Engel, K. Kruger, S. O'Doherty and W.T.  
536 Sturges, Ozone-depleting substances (ODSs) and related chemicals, Chapter 1 in  
537 *Scientific Assessment of Ozone Depletion: 2010*, Global Ozone Research and Monitoring  
538 Project – Report No. 52, World Meteorological Organization, Geneva, Switzerland, 2011.

539 Navarro, M.A., E.L. Atlas, A. Saiz-Lopez, X. Rodriguez-Lloveras, D.E. Kinnison, J.-F.  
540 Lamarque, S. Tilmes, M. Filus, N.R.P. Harris, E. Meneguz, M.J. Ashfold, A.J. Manning,  
541 C.A. Cuevas, S.M. Schauffler and V. Donets, Airborne measurements of organic bromine  
542 compounds in the Pacific tropical tropopause layer, *Proc. Natl. Acad. Sci. USA*, **112**, 13789-  
543 13793, doi:10.1073/pnas.1511463112, 2015.

544 Nolan Sherry Associates (NSA) proprietary information: some of the data used in these  
545 calculations is proprietary in nature, being based on direct information from discussions  
546 with the producers and have been aggregated for reasons of confidentiality. In the case of  
547 the HCFC-22 production data this is also because there are two uses of HCFC22; as a  
548 chemical intermediate, and as a refrigerant and a foam blowing agent. The latter uses are  
549 "emissive" and are controlled by the Montreal Protocol (<http://ozone.unep.org>) and are in  
550 the public domain. Information on the controlled uses of HCFC-22 may be found on this  
551 website, or by access to the Multilateral Fund of the Montreal Protocol  
552 (<http://www.multilateralfund.org>), and, in the case of China, by private subscription to the  
553 industry magazine China Fluoride Materials ([www.cnchemicals.com](http://www.cnchemicals.com)).

554 Pisso, I., P.H. Haynes and K.S. Law, Emission location dependent ozone depletion potentials  
555 for very short-lived halogenated species *Atmos., Chem. Phys.*, **10**, 12025-12036, 2010.

556 Randel, W.J., M. Park, L. Emmons, D. Kinnison, P. Bernarth, K.A. Walker, C. Boone and H.  
557 Pumphrey, Asian monsoon transport of pollution to the stratosphere, *Science*, **328**, 611-  
558 613, 10.1126/science.1182274, 2010.

559 Sala, S. H. Bönisch, T. Keber, D.E. Oram, G. Mills and A. Engel, Deriving an atmospheric  
560 budget of total organic bromine using airborne in-situ measurements from the Western  
561 Pacific during SHIVA, *Atmos. Chem. Phys.* **14**, 6903-6923, doi:10.5194/acp-14-6903-2014.

562 Shao, M., D. Huang, D. Gu, S. Lu, C. Chang and J. Wang, Estimate of anthropogenic  
563 halocarbon emission based on measured ratio relative to CO in the Pearl River Delta  
564 region, China, *Atmos. Chem. Phys.*, **11**, 5011-5025, doi:10.5194/acp-11-5011-2011.

565 Simmonds, P. G., Manning, A. J., Cunnold, D. M., McCulloch, A., O'Doherty, S., Derwent, R.  
566 G., Krummel, P. B., Fraser, P. J., Dunse, B., Porter, L. W., Wang, R. H. J., Grealley, B. R.,  
567 Miller, B. R., Salameh, P., Weiss, R. F. and Prinn, R. G.: Global trends, seasonal cycles,  
568 and European emissions of dichloromethane, trichloroethene, and tetrachloroethene from  
569 the AGAGE observations at Mace Head, Ireland, and Cape Grim, Tasmania, *J. Geophys.*  
570 *Res.*, **111** (D18304), doi:10.1029/2006JD007082, 2006.

571 Simpson, I.J., S.K. Akagi, B. Barletta, N.J. Blake, Y. Choi, G.S. Diskin, A. Fried, H.E. Fuelberg,  
572 S. Meinardi, F.S. Rowland, S.A. Vay, A.J. Weinheimer, P.O. Wennberg, P. Wiebring, A.  
573 Wisthaler, M. Yang, R.J. Yokelson and D.R. Blake, Boreal forest fire emissions in fresh  
574 Canadian smoke plumes: C1-C10 volatile organic compounds (VOCs), CO<sub>2</sub>, CO, NO<sub>2</sub>, NO,  
575 HCN and CH<sub>3</sub>CN, *Atmos. Phys. Chem.*, **11**, 6445-6463, 2011.

576 Singh, H.B., L.J. Salas, A.J. Smith and H. Shigeishi, Measurements of some potentially  
577 hazardous organic chemicals in urban environments, *Atmos. Environ.*, **15**, 601-612, 1981.

578 Sinnhuber, B.-M., N. Sheode, M. Sinnhuber, M.P. Chipperfield and W. Feng, The contribution  
579 of anthropogenic bromine emissions to past stratospheric ozone trends: a modelling study,  
580 *Atmos. Phys. Chem.*, **9**, 2863-2871, 2009.

581 SPARC, 2016: SPARC Report on the Mystery of Carbon Tetrachloride, Q. Liang, P.A.  
582 Newman, and S. Reimann (Eds.), SPARC Report No. 7, WCRP-13/2016, available  
583 at [www.sparc-climate.org/publications/sparc-reports/sparc-report-no7](http://www.sparc-climate.org/publications/sparc-reports/sparc-report-no7).

584 Worton, D. R., Sturges, W. T., Schwander, J., Mulvaney, R., Barnola, J.-M. and Chappellaz,  
585 J.: 20<sup>th</sup> century trends and budget implications of chloroform and related tri- and  
586 dihalomethanes inferred from firn air, *Atmos. Chem. Phys.*, **6**, 2847-2863, doi:10.5194/acp-  
587 6-2847-2006, 2006.

588 Xue, L., T. Wang, I.J. Simpson, A. Ding, J. Gao, D.R. Blake, X. Wang, W. Wang, H. Lei and  
589 D. Jin, Vertical distributions of non-methane hydrocarbons and halocarbons in the lower  
590 troposphere over northeast China, *Atmos. Environ.*, **45**, 6501-6509, 2011.

591 Zhang, Y., Sperber, K. R., and Boyle, J. S.: Climatology and interannual variation of the East  
592 Asian winter monsoon: Results from the 1979–95 NCEP/NCAR Reanalysis, *Monthly*  
593 *Weather Review*, **125**, 2605–2619, doi:10.1175/1520-  
594 0493(1997)125<2605:CAIVOT>2.0.CO;2, 1997.

595

## 596 **Acknowledgements**

597

598 The authors would like to thank our CARIBIC project partners and the CARIBIC technical team  
599 (in particular C. Koeppel, D. Scharffe). The Malaysia and Taiwan activities were funded  
600 through the UK Natural Environment Research Council (NERC) International Opportunities  
601 Fund (NE/J016012/1, NE/J016047/1, NE/N006836/1). CARIBIC has become part of IAGOS  
602 ([www.IAGOS.org](http://www.IAGOS.org)) and is supported by the German Ministry of Education and Science and  
603 Lufthansa. The CARIBIC halocarbon measurements were part-funded by the European FP7  
604 project SHIVA (226224). UM-BMRS is supported by the Malaysian Ministry of Higher  
605 Education (Grant MOHE-HICoE IOES-2014). The sampling at Hengchun and Fuguei Cape  
606 was operated under the Seven South East Asian Studies (7-SEAS) program and funded by  
607 Taiwan EPA and MOST. J.L and L.G. were funded through a NERC fellowship  
608 (NE/1021918/1) and studentship (NE/1210143) respectively. We acknowledge use of the  
609 NAME atmospheric dispersion model and associated NWP meteorological data sets made  
610 available to us by the UK Met Office. We also acknowledge the significant storage resources  
611 and analysis facilities made available to us on JASMIN by STFC CEDA along with the  
612 corresponding support teams.

613

614

615

616 **Table 1:** Summary of Cl-VSLS data from the 3 surface stations and the 7 CARIBIC flights. For  
617 comparison, the ranges reported in the most recent WMO Ozone Assessment (Carpenter and  
618 Reimann et al., 2015) for the marine boundary layer (MBL) and lower Tropical Tropopause  
619 Layer (TTL, 12-14 km altitude) are also shown. All data are reported as mole fractions (ppt).

620

621 **Figure 1:** Map of the region showing the location of each CARIBIC sample. The markers have  
622 been coloured according to their CH<sub>2</sub>Cl<sub>2</sub> concentration to highlight the regions where  
623 enhanced levels of VSLS were observed. Also shown are the approximate locations of the 3  
624 surface stations (orange crosses).

625

626 **Figure 2:**

627 *Upper panel (a):* Mole fractions (ppt) of the 4 chlorinated VSLS in air samples collected at  
628 Cape Fuguei, Taiwan in March/April 2014. The error bars are  $\pm 1$  standard deviation. The  
629 black arrows show the dates of the footprint maps shown below.

630 *Lower panel (b-d):* NAME footprint maps indicating the likely origin of the air sampled at Cape  
631 Fuguei. Figures (b, 13 March) and (c, 30 March) show examples where the observed VSLS  
632 levels are very high and suggest a strong influence from continental East Asia. Figure (d) is  
633 from 29 March where the influence of the mainland is much lower and the VSLS mole fractions  
634 are much closer to the expected background level.

635 The location of Cape Fuguei is indicated with a blue circle (see also Figure 1).

636

637 **Figure 3:**

638 *Upper panel (a):* Mole fractions (ppt) of the 4 chlorinated VSLS in air samples collected at  
639 Bachok in Jan/Feb 2014. Strongly enhanced levels of all 4 compounds were seen for a 7-  
640 day period at the beginning of the campaign (20-26 Jan). Also shown (dashed line) are the  
641 approximate median background concentrations in the remote marine boundary layer in  
642 2012 (from Carpenter and Reimann et al., 2015).

643 *Lower panels (b-f):* NAME footprint maps indicating the likely origin of the air sampled at  
644 Bachok. During the pollution episode (b = 21 Jan; c = 23 Jan; d = 24 Jan) the samples would  
645 have been heavily impacted by emissions from the East Asian mainland, whilst this influence  
646 is much reduced during the cleaner, non-polluted periods (e = 3 Feb; f = 5 Feb). Note that  
647 even after the main pollution event, the abundance of the VSLS remain significantly above  
648 true background levels for much of the time, suggesting a widespread influence from  
649 industrial emissions on a regional scale.

650 The location of Bachok is indicated with a blue circle (see also Figure 1).

651 **Figure 4:**

652 (a) Time-series of the modelled carbon monoxide (CO) anomaly at Bachok (i.e. that due only  
653 to industrial emissions from north of 20°N in the previous 12 days) for winter 2013/14. The  
654 CH<sub>2</sub>Cl<sub>2</sub> data (grey squares) from the Bachok sampling period are overlaid. The dashed lines  
655 show the 25 ppb and 50 ppb thresholds referred to in 3c (see supplement for further details).

656 (b) Correlation of the modelled CO anomaly with the observed CH<sub>2</sub>Cl<sub>2</sub>.

657 (c) Average number of days each month, averaged over six consecutive winters (2009/10 –  
658 2014/15) where the modelled carbon monoxide anomaly at Bachok is above a particular

659 threshold (25 ppb and 50 ppb which, from the regression in 3b, correspond to 176 ppt and  
660 315 ppt of  $\text{CH}_2\text{Cl}_2$ ). The 2013/14 winter is shown separately for comparison with the 6-year  
661 average.

662 **Figure 5**

663 (a) Mole fractions (ppt) of  $\text{CH}_2\text{Cl}_2$  in CARIBIC air samples collected at 10-12km altitude over  
664 Northern India, the Bay of Bengal and SE Asia. The samples are plotted against longitude  
665 and have been coloured by date.

666 (b) Mole fraction (ppt) of  $\text{CH}_2\text{ClCH}_2\text{Cl}$  in selected CARIBIC samples (note:  $\text{CH}_2\text{ClCH}_2\text{Cl}$  was  
667 not monitored in the samples collected between Bangkok to Kuala Lumpur, and only in a  
668 selection of samples on the Frankfurt-Bangkok route).

669 (c) Total Cl-VSLS derived from the 4 compounds of interest in the CARIBIC samples (note:  
670 total Cl-VSLS could only be calculated for the samples shown in Fig 5b above).

671 (d) NAME footprint maps indicating the likely origin of the air sampled by the CARIBIC  
672 aircraft. NAME footprints at this altitude, and particularly in regions of strong sub-grid-scale  
673 convection not captured fully in the gridded meteorological input data, may be less reliable  
674 than those at the surface sites. This makes pinpointing particular emission regions more  
675 difficult. The central panel therefore shows a composite footprint derived from the samples  
676 that contained the highest levels of  $\text{CH}_2\text{Cl}_2$  (90<sup>th</sup> percentile,  $[\text{CH}_2\text{Cl}_2] > 75.6$  ppt), with the  
677 composite footprint from the remaining samples ( $[\text{CH}_2\text{Cl}_2] < 75.6$  ppt) shown in the left hand  
678 panel. To emphasise the likely source regions the right hand panel shows the difference  
679 between the middle and left hand panels. The geographical location of each sample  
680 included in the composite analysis are shown in blue circles.

681 **Table 1**

682

	Taiwan 2013		Taiwan 2014		Bachok 2014			MBL (WMO 2014) <sup>(b)</sup>	
	Median	Range	Median	Range	Median (CS) <sup>(a)</sup>	Median (non-CS)	Range	Median	Range
<b>CH<sub>2</sub>Cl<sub>2</sub></b>	226.6	68 - 624	227.4	70 - 639	170.4	81.9	64.8 - 355	<b>28.4</b>	<b>21.8 - 34.4</b>
<b>CH<sub>2</sub>ClCH<sub>2</sub>Cl</b>	-	-	85.4	16.7 - 309	62.2	21.7	16.4 - 120 <sup>(c)</sup>	<b>3.7</b>	<b>0.7 - 14.5<sup>(d)</sup></b>
<b>CHCl<sub>3</sub></b>	33.0	11.6 - 232	35.1	13.8 - 103	22.8	14.7	12.8 - 30.5	<b>7.5</b>	<b>7.3 - 7.8</b>
<b>C<sub>2</sub>Cl<sub>4</sub></b>	4.4	1.7 - 16.6	5.5	1.7 - 18.6	4.5	1.9	1.5 - 9.5	<b>1.3</b>	<b>0.8 - 1.7</b>
<b>Σ Cl<sub>VLSL</sub></b>	-	-	755.8	232 - 2178	546.0	243.1	207 - 1078 <sup>(c)</sup>	<b>93.4</b>	<b>70 - 134</b>

683

684

	CARIBIC (FRA-BKK, 65-97°E)			CARIBIC (BKK-KUL, 100-105°E)			Lower TTL (WMO 2014) <sup>(b)</sup>	
	10-12 km			10-12 km			12-14 km	
	Mean	Median	Range	Mean	Median	Range	Mean	Range
<b>CH<sub>2</sub>Cl<sub>2</sub></b>	43.2	31.6	14.6 - 121	50.4	46.5	22.5 - 100	<b>17.1</b>	<b>7.8 - 38.1</b>
<b>CH<sub>2</sub>ClCH<sub>2</sub>Cl<sup>(e)</sup></b>	9.9	6.1	0.4 - 29.1	-	-	-	<b>3.6</b>	<b>0.8 - 7.0</b>
<b>CHCl<sub>3</sub></b>	7.0	6.0	2.0 - 15.6	9.3	8.7	3.7 - 46.6	<b>6.8</b>	<b>5.3 - 8.2</b>
<b>C<sub>2</sub>Cl<sub>4</sub></b>	0.87	0.65	0.1 - 4.4	1.6	1.5	0.2 - 5.9	<b>1.1</b>	<b>0.7 - 1.3</b>
<b>Σ Cl<sub>VLSL</sub><sup>(e)</sup></b>	153.7	119.3	48.4 - 330				<b>67</b>	<b>36 - 103</b>
<b>Σ Cl<sub>VLSL</sub>*<sup>(f)</sup></b>	110.9	81.4	35.2 - 301	134.8	127.8	56.6 - 251	-	-

685

686

687 <sup>(a)</sup> CS and non-CS refer to the cold surge (polluted) and non-cold surge periods at Bachok688 <sup>(b)</sup> The WMO data is a compilation of all reported global measurements up to, and including, the year 2012. The  
689 range represents the smallest mean minus one standard deviation and the largest mean plus one standard  
690 deviation of all considered datasets. Data from the TTL was derived from various aircraft and balloon  
691 campaigns.692 <sup>(c)</sup> CH<sub>2</sub>ClCH<sub>2</sub>Cl was only analysed for in 16 of the 28 samples collected at Bachok693 <sup>(d)</sup> Note that the CH<sub>2</sub>ClCH<sub>2</sub>Cl MBL data actually date back to the early 2000s. No recent data was reported.694 <sup>(e)</sup> CH<sub>2</sub>ClCH<sub>2</sub>Cl was only analysed for in selected samples from the Frankfurt-Bangkok flights and in no samples  
695 collected during the Bangkok-Kuala Lumpur flights. These statistics are therefore based on a reduced number  
696 of samples on the FRA-BKK route (24 out of 98).697 <sup>(f)</sup> Σ Cl<sub>VLSL</sub>\* is defined as the sum of Cl-VLSL excluding the contribution from CH<sub>2</sub>ClCH<sub>2</sub>Cl. Statistics derived from  
698 all samples (98 FRA-BKK; 81 BKK-KUL).

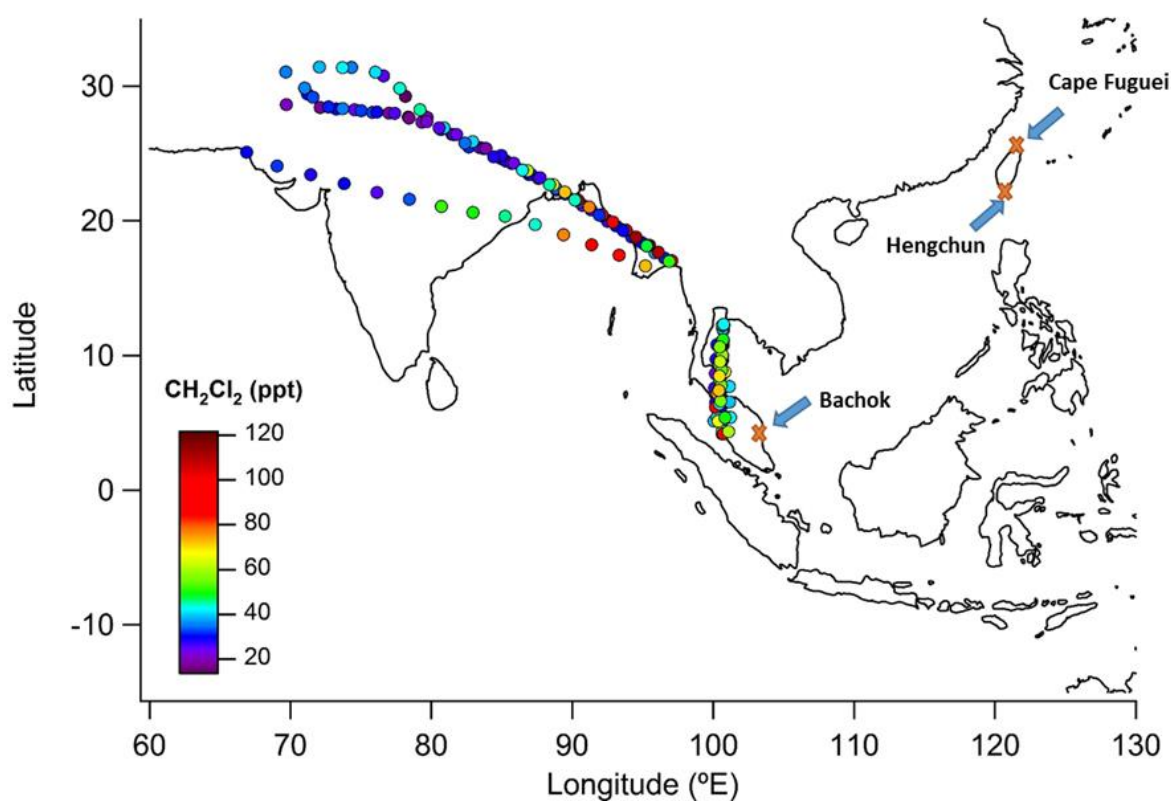
699

700

701



702 **Figure 1**  
703  
704  
705

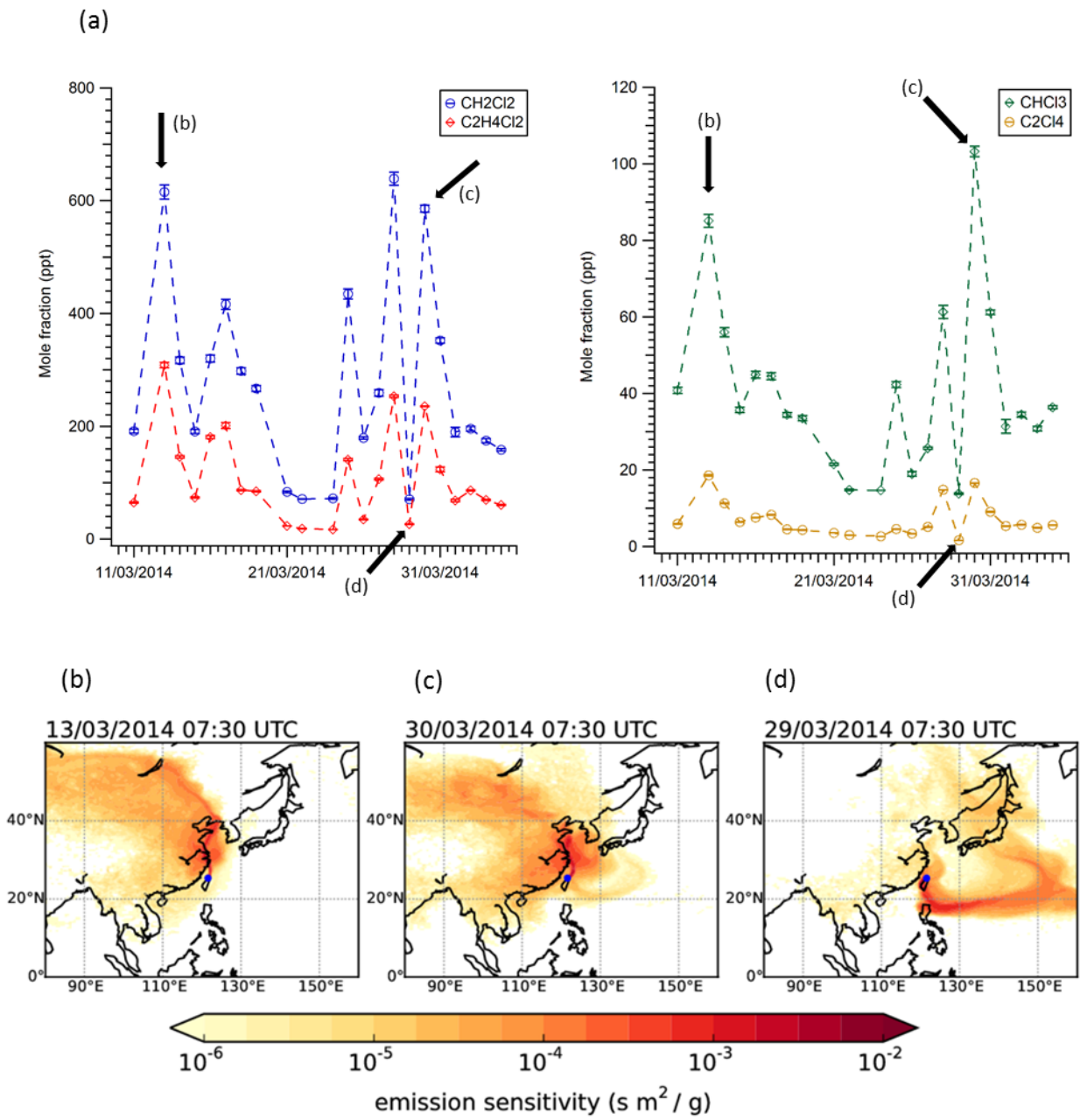


706  
707  
708  
709  
710  
711  
712

713 **Figure 2**

714

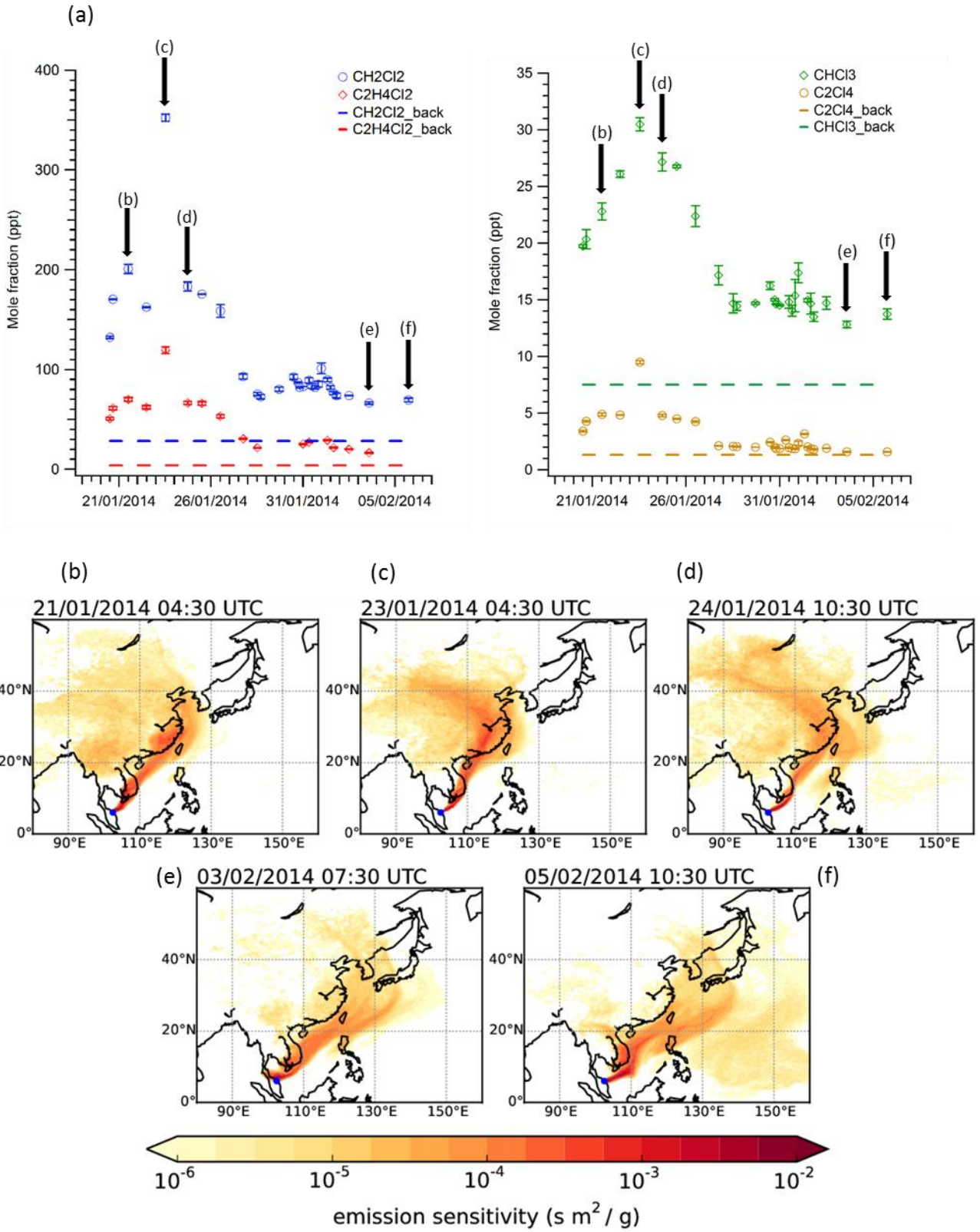
715



716

717

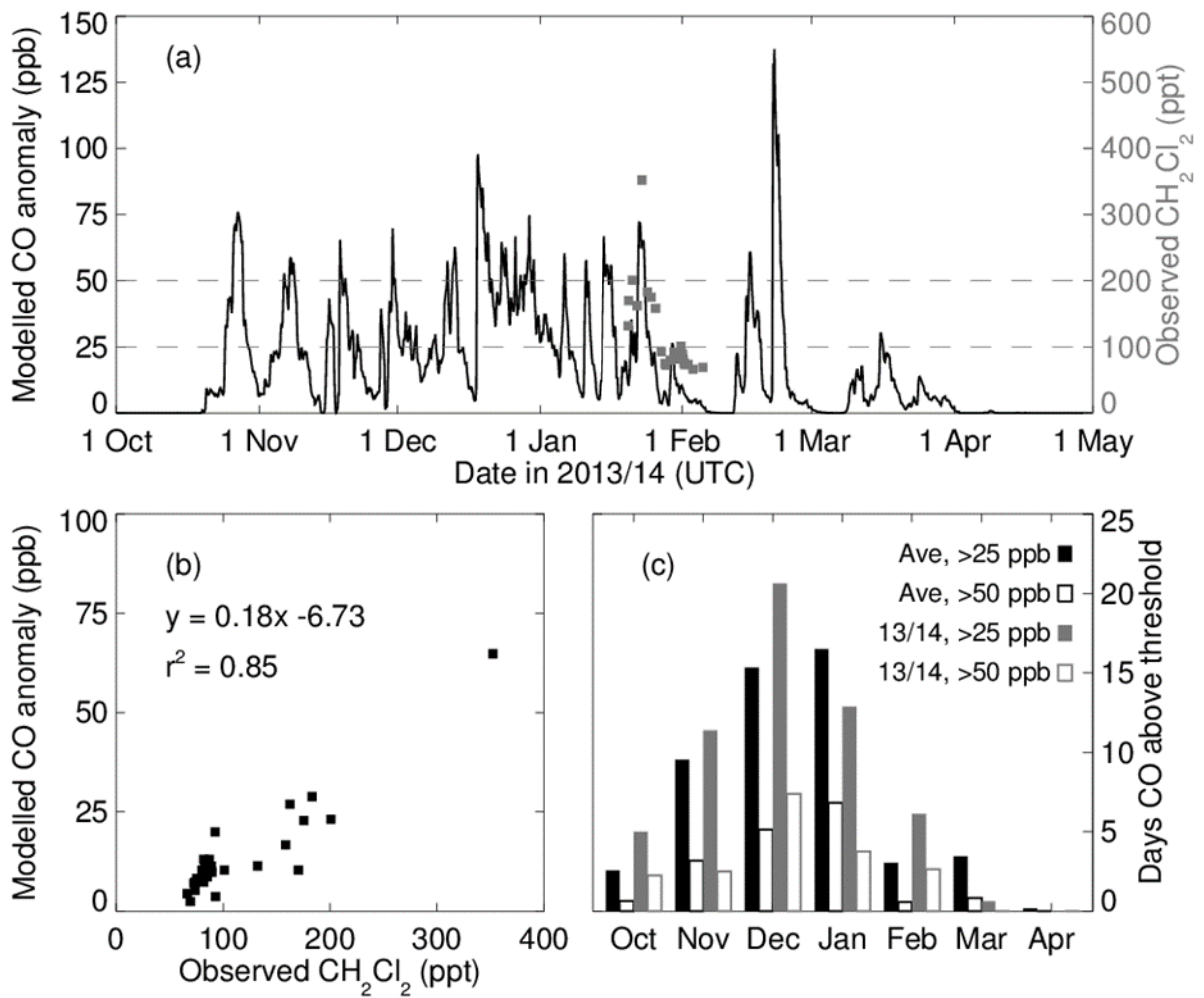
718 **Figure 3**  
 719



720  
 721  
 722  
 723

724 **Figure 4**

725  
726  
727

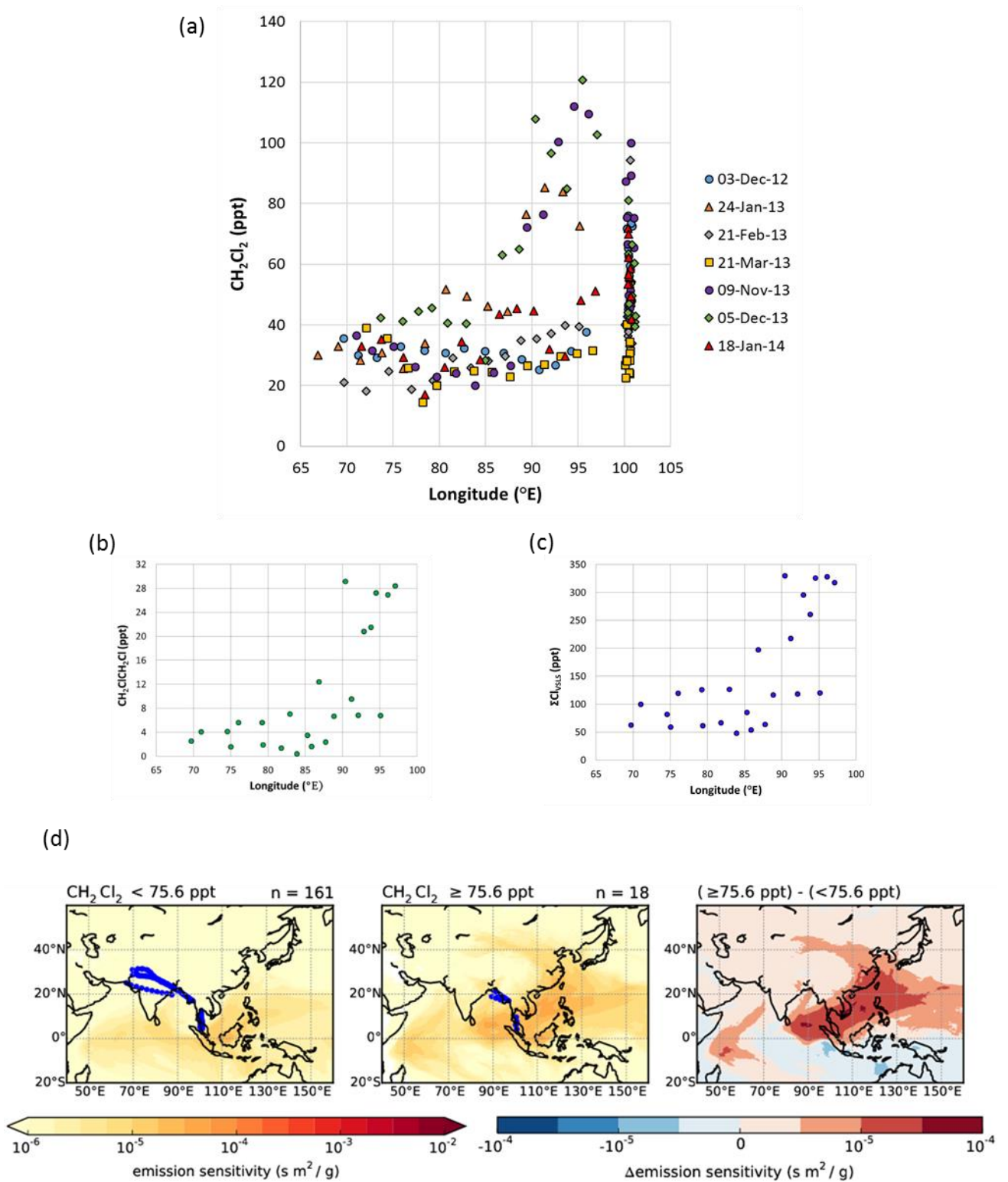


728  
729  
730  
731  
732

733 **Figure 5**

734

735



736

737

738